Int. J. Electrochem. Sci., 7 **(2012)** 785 - 805

International Journal of
ELECTROCHEMICAL
SCIENCE
www.electrochemsci.org

Determination of the diffusion coefficients for charge transfer through homo-, bilayered- and co-polymers of 3-methyl-thiophene and N-methylpyrrole.

Nada F. Atta[*], *Ahmed Galal* , *Shimaa M. Ali*

Department of chemistry, Faculty of science, Cairo University, Postal code 12613, Giza, Egypt
[*]E-mail: nada_fah1@yahoo.com

Received: 8 October 2011 / *Accepted:* 25 November 2011 / *Published:* 1 January 2012

Conducting homo-, bilayered- and co-polymers of 3-methylthiophene (MT) and N-methylpyrrole (NMPy) were electrochemically deposited on platinum electrode. Electrochemical investigation of the resulting films was achieved using cyclic voltammetry and chronocoulometry. The diffusion coefficients were calculated in case of using different films of different thicknesses. The synthesis and testing the films in presence of different types of electrolytes and solvents were studied. The results showed that a memory effect caused by the synthesis anion affects further interaction between the film and the test anion which consequently affect the diffusion coefficient. The charge spacing effect caused by the type of electrolyte is more pronounced in the case of PMPy compared to PMT. Also, diffusion coefficient values were calculated for films with different thickness prepared from different monomers feed ratios in different electrolytes and solvents. Some of them showed similar trend to the homo-polymers. For conducting bilayers, the inner layer influences the redox process of the bilayer. This can be showed from the cyclic voltammetry measurements and diffusion coefficient calculations. FTIR measurements proved the incorporation of both individual monomers in the copolymer films. TGA proved that the thermal stability of the copolymer increased by increasing NMPy content. On the other hand, surface morphology revealed by SEM showed a distinct difference between homo- and co-polymeric structures.

Keywords: Conducting polymers, bilayers, copolymers, diffusion coefficients, FTIR, TGA, SEM

1. INTRODUCTION

Conducting polymers are very interesting materials. They have a wide variety of many useful applications in optic or electronic devices, batteries and catalysis. They also offer outstanding properties as sensitive layers in electrochemical analytical devices. Not only simple single polymeric layers coated on electrodes but also copolymers and bilayers of conducting polymers exhibit

interesting properties. The properties of bilayers of redox polymers were first investigated by Murray [1, 2] who discovered that the oxidation or reduction of the outer film is mediated by the inner one. Later, bilayers of conducting polymers composed of poly(pyrrole)/poly(bithiophene) and poly(bithiophene) /poly(pyrrole) were studied by Torres and Fox [3]. It was found that the outer layer film can be oxidized only if the inner one is in a conducting state. Other papers also demonstrated that the electrochemical behavior of the bilayer was predominantly determined by the inner layer redox characteristics [4-7]. On the other hand, copolymers of MT and 3-octylthiophene were studied by Pei [8] and the results showed that the copolymer stability was higher as MT content increased. Poly(MT-co-pyrrole) was prepared and studied [9, 10]. It was discovered that pyrrole was the major component of the prepared copolymer and the electrical conductivity of the copolymer was higher than that of the individual poly(pyrrole), owing to increasing porosity. Also, copolymers composed of pyrrole and NMPy synthesized and conductivity measurements were performed [11]. It was found that the conductivity of the film decreased with increasing proportion of NMPy in the copolymer.

Charge transfer through electroactive polymer films was believed to occur via an electron hopping process [12]. This process was governed by the mundane laws of Fickian diffusion for a variety of different polymer films. Thus, thin-layer electrochemistry can be applied to the polymer film experiment. For example, the diffusion coefficient can be derived from chronocoulometric charge vs. time curve. In the determination of the diffusion coefficient values for some conducting polymers [13, 14], it was found that charge transfer occurs at the polymer/solution interface and not at the inner electrode substrate surface after diffusion through the polymer matrix. In other words, the charge transfer was predominantly diffusion-controlled at the polymer/solution interface.

In this work, the diffusion coefficients for homo-PMT and PMPy were determined. The effect of changing some factors such as the film thickness, the synthesis and characterization electrolytes and the characterization solvent will be studied. Moreover, this study will be extended to bilayers and copolymers prepared from these monomers and further spectroscopic, structural, thermal and surface characterization will be presented.

2. EXPERIMENTAL

2.1. Chemicals and electrochemical cells

All chemicals were used as received without further purification. 3-methyl thiophene, N-methylpyrrole, tetrabutyl ammonium hexafluorophosphate, lithium perchlorate and acetonitrile were obtained from Aldrich (Milwankee, USA). Aqueous solutions were prepared using double-distilled water.

Electrochemical polymerization and characterizations were carried out with a three-electrodes/one-compartment glass cell. The working electrode was platinum disc (diameter: 1.5 mm). The auxiliary electrode was in the form of 6.0 cm platinum wire. All the potentials in the polymerization and the voltammetric studies were referenced to a saturated Ag/AgCl electrode. The working electrode was mechanically polished using an alumina (2 μm)/ water slurry until no visible

scratches were observed. Prior to immersion in the cell, the electrode surface was thoroughly rinsed with distilled water and dried. All experiments were performed at 25 °C.

2.2. Equipments and techniques

The electrosynthesis of the polymers and their electrochemical characterization were performed using a BAS-100B electrochemical analyzer (BAS, West Lafayette, USA). Homo-, bilayered- and co-polymers were electrochemically formed by repeatedly cycling the potential of the working electrode between two limits as will be indicated in the "Results and discussion" section. The IR transmission spectra were obtained on a Brucker Vector 22, Germany and Jasco FTIR 460 plus Japan spectrometer. Thermal gravimetric analysis was performed using a Shimadzu TGA-50H instrument. Philibs XL 30 instrument was used to obtain the scanning electron micrographs of the polymer films.

3. RESULTS AND DISCUSSION

3.1. Electrochemical polymerization of MT

The electro-polymerization of MT can be achieved in a three-electrode, one compartment electrochemical cell. The potential applied between the platinum disc-working electrode and the reference Ag/AgCl is varied with time, namely 100 $mV.s^{-1}$, between two potential limits, ca. E_i=-0.2 V and E_f=+1.8 V. The thickness of the resulting polymer film is therefore controlled by the number of repeated cycles scanned. Figure 1a shows the repeated cyclic voltammograms for 5 cycles during the electro-polymerization of MT. The electrolyte solution contains 0.05 M MT, and 0.05 M $TBAPF_6$ in acetonitrile.

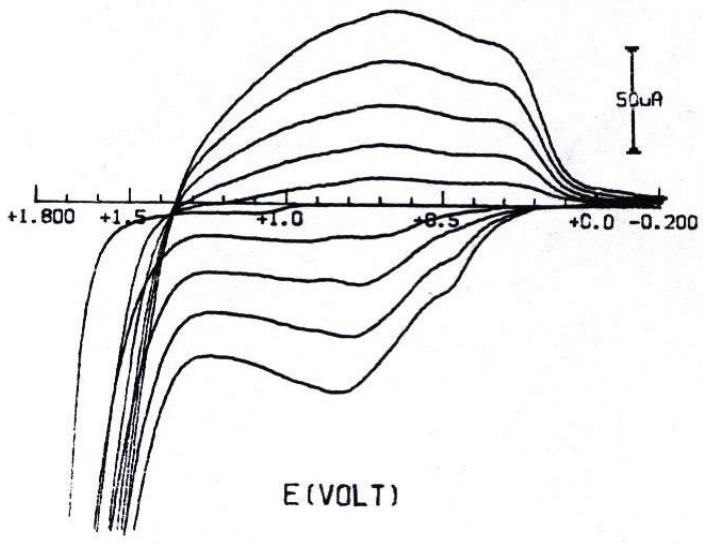

Figure 1a. Repeated cyclic voltammogrames for the formation of PMT on Pt. Electrolyte: 0.05 M MT, 0.05 M $TBAPF_6$ in AcN, scan rate=100 $mV.s^{-1}$, E_i=-0.2 V, E_f=+1.8 V for 5 cycles

Successive scans show an increase in current caused by the oxidation process that is responsible for the polymer film thickening with the appearance of distinctive shoulder around +0.5 V. The sharp increase in current at the end of the anodic scan shifts to less positive potential values could be attributed to the electro-catalytic activity of the surface that improves with the film thickening. On the other hand, the reverse scan is characterized by a broad peak followed by a second shoulder.

3.2. Electrochemical characterization of PMT

PMT was characterized in the monomer free solution by cyclic voltammetry. Figure 1b shows the cyclic voltammetric response of PMT films formed with different thicknesses using repeated cyclic voltammetry (3, 5, and 10 cycles) as in curves a, b, and c, respectively. The voltammograms of Figure 1b show that current response increases with thickness. This is attributed to the increase in the number of active sites responsible for anion exchange. Moreover, the amount of dopants exchanged during the oxidation-reduction switching of the film increases. This is a logical consequence of the increased capacity of the film. The potential limits used during cycling (ca. E_i=-0.2 V and E_f=+1.2 V) indicate that the polymer film is cycled between its oxidized (doped) and reduced (undoped) states. A broad oxidation peak is shown, that is more manifested for relatively thick films. On the other hand, the reduction process is a more complicated process compared to the oxidation (doping) step. Therefore, an even much broader reduction peak is observed for reduction with the appearance of a well defined shoulder at a negative potential. After the polymer film was first cycled in a monomer free solution, it has been also characterized by chronocoulometry.

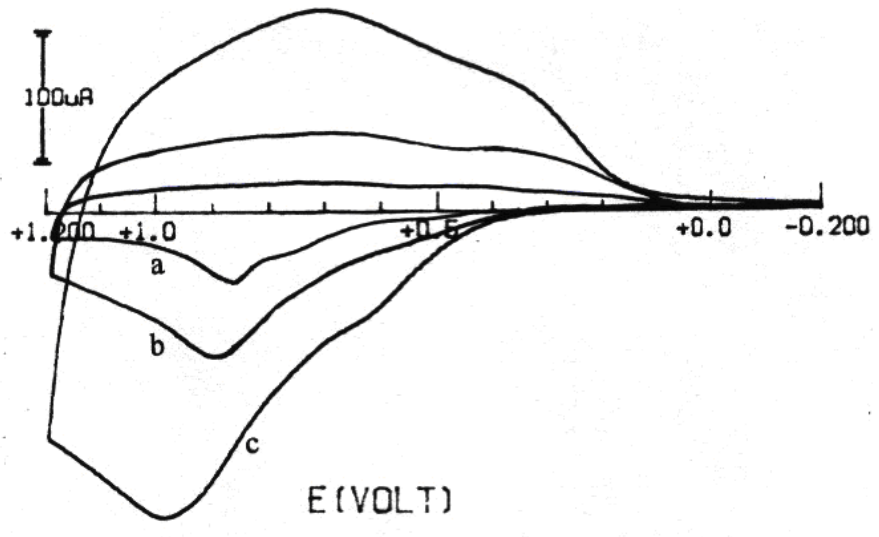

Figure 1b. Cyclic voltammogram of PMT formed by repeated cycles; 3 cycles (a), 5 cycles (b) and 10 cycles (c) in 0.05M $TBAPF_6$ in AcN. Scan rate=100 $mV.s^{-1}$, E_i=-0.2 V, E_f=+1.2 V.

The excitation signal in chronocoulometry is a square-wave voltage signal. The potential of the working electrode is stepped from a value at which no faradaic current occurs, E_i, to a potential, E_s, at which the surface concentration of the electro-active species is effectively zero. Finally, the potential is maintained at E_s until the end of the experiment or be stepped to a final potential E_f after some interval of time τ has passed [15]. A typical set of experimental results are displayed in Figure 1c (the cyclic voltammograms shown in Figure 1b, curves a, b, and c, were used to determine the potential limits for chronocoulometric experimental conditions).

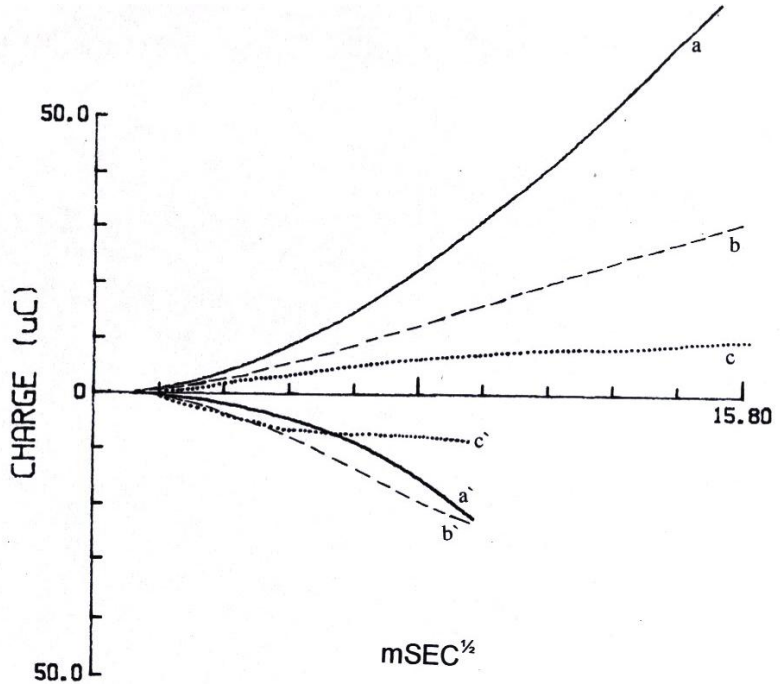

Figure 1c. Chronocoulometry experiment for PMT films formed by repeated cycles (···) 3 cycles, (---) 5 cycles, and (—) 10 cycles. a, b, c, and a`, b`, c` for the forward and reverse steps, respectively.

In a typical chronocoulometric experiment the current decays smoothly and approaches zero with time as described by the Cottrel equation [15]:

$$i_t = \frac{2\,n\,F\,A\,C\,D^{1/2}\,t^{1/2}}{\pi^{1/2}} \qquad (1)$$

Where i_t is the current at time t, n is the number of electrons, F is the Faraday's constant, A is the electrode area, C is the concentration of oxidized/reduced species, and D is the diffusion coefficient. The measured charge (or the integrated resulting current) from the potential step represents contributions from:

- Doping of anions (during the oxidation step) at a rate that is controlled by diffusion.
- Electrolysis of an electro-active species that is adsorbed on the electrode surface.

- The charging of electrode-electrolyte double-layer capacitance.

The three charge-components can be expressed as follows:

$$Q_{total} = \int_0^t i.dt \qquad (2a)$$

$$Q_{total} = \frac{2\,n\,F\,A\,C\,D^{1/2}\,t^{1/2}}{\pi^{1/2}} + n\,F\,A\,\Gamma + Q_{dl} \qquad (2b)$$

where, Γ is the amount of adsorbed reactant. The second and third terms will be considered the same for different films by approximation. Thus, from the slope of the Q vs. $t^{1/2}$ relation, the diffusion coefficient can be estimated. Table 1 summarizes the values of the diffusion coefficients for PMT grown potentiostatically for different thicknesses. The electrolytes used during synthesis are 0.05 M $TBAPF_6$ or 0.05 M $LiClO_4$ in AcN. The test solution contains 0.05 M $TBAPF_6$/AcN or 0.05 M $LiClO_4$/AcN or 0.05 M $LiClO_4/H_2O$. The measurements were recorded around the peak that appeared in the corresponding cyclic voltammogram for the forward cycle (Figures 1b). The calculated values of diffusion coefficients, presented in Table 1, were close to those calculated by Juttner et al. [16] for PMT (10^{-9} cm^2/s) and Tezuka et al. [17] for polythiophene ($3x10^{-10}$ cm^2/s).

Table 1. Values of diffusion coefficients, D (cm^2/s), calculated from the double-potential experiments and using Cottrel equation (1). PMT formed with different thickness (3, 5, 10 cycles) in AcN.

PMT	3 Cycles	5 Cycles	10 Cycles
$TBAPF_6/TBAPF_6/AcN$*	$2.920x10^{-8}$	$1.521x10^{-7}$	$3.738x10^{-7}$
$TBAPF_6/LiClO_4/AcN$*	$4.197x10^{-8}$	$1.293x10^{-7}$	$3.386x10^{-7}$
$LiClO_4/LiClO_4/AcN$*	$6.993x10^{-8}$	$1.653x10^{-7}$	$2.571x10^{-7}$
$LiClO_4/TBAPF_6/AcN$*	$5.188x10^{-8}$	$1.084x10^{-7}$	$2.353x10^{-7}$
$LiClO_4/LiClO_4/H_2O$*	$4.479x10^{-9}$	$1.721x10^{-8}$	$5.816x10^{-8}$
$TBAPF_6/LiClO_4/H_2O$*	$1.149x10^{-8}$	$1.752x10^{-8}$	$8.450x10^{-8}$

* Synthesis electrolyte/test electrolyte/test solvent

The following observations could be withdrawn from the data of Table 1:

- Thicker films exhibit large D values for those calculated for the forward (doping) and reverse (undoping) processes around the peak. It is important to notice that changing the type of electrolyte and/or solvent has no effect on this result. Therefore, the increase in thickness results in an increase in the loading capacity of the dopant within the film. Also, the possible existence of channels in relatively thicker films contributes to the increase of electrolyte interaction with the inner fibers in the film.
- When comparing films prepared in $TBAPF_6$/AcN then tested in the same electrolyte or $LiClO_4$/AcN, the value of D slightly increases. On the other hand, the corresponding D values slightly decrease when the films are synthesized in $LiClO_4$/AcN and tested in $TBAPF_6$/AcN compared to those

tested in $LiClO_4$/AcN. This could be explained by the "memory effect" caused by the synthesis anion and affect further interaction between the film and the test anion. In conclusion, the increase in charge to size of test anion compared to that of synthesis anion shows slight increase in *D* values

- Films tested in $LiClO_4/H_2O$ show relatively low *D* values compared to those tested in AcN. The hydrophobic nature of PMT films explains the hindrance of diffusion of the solvated anions in this case.

3.3. Electrochemical polymerization of NMPy

The electropolymerization of NMPy was achieved by repeated CV as described previously. Figures 2a shows the repeated CV of a Pt electrode in 0.05 M NMPy, 0.05 M $TBAPF_6$/AcN.

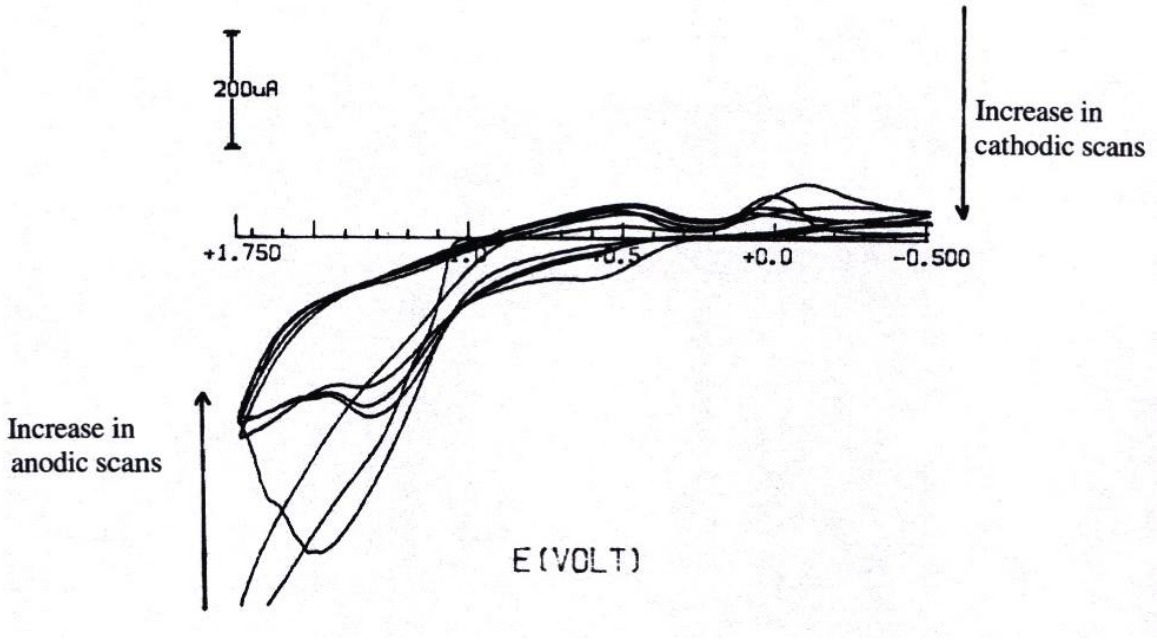

Figure 2a. Repeated cyclic voltammogrames for the formation of PMPy on Pt. Electrolyte: 0.05 M NMPy, 0.05 M $TBAPF_6$ in AcN, scan rate=100 $mV.s^{-1}$, E_i=-0.5 V, E_f=+1.75 V for 5 cycles.

A distinctive difference could be noticed when comparing Figure 2a with that for MT Figure1a. PMPy is less conductive in nature when compared to PMT. The insulating character of PMPy film is reflected by the decrease in current as the number of scans increases.

3.4. Electrochemical characterization of PMPy

Figure 2b shows the cyclic voltammograms of PMPy synthesized in $TBAPF_6$/AcN and tested in $TBAPF_6$/AcN, $TBAPF_6$/AcN tested in $LiClO_4$/AcN, and $LiClO_4$/AcN tested in $TBAPF_6$/AcN as in curves a, b, and c, respectively.

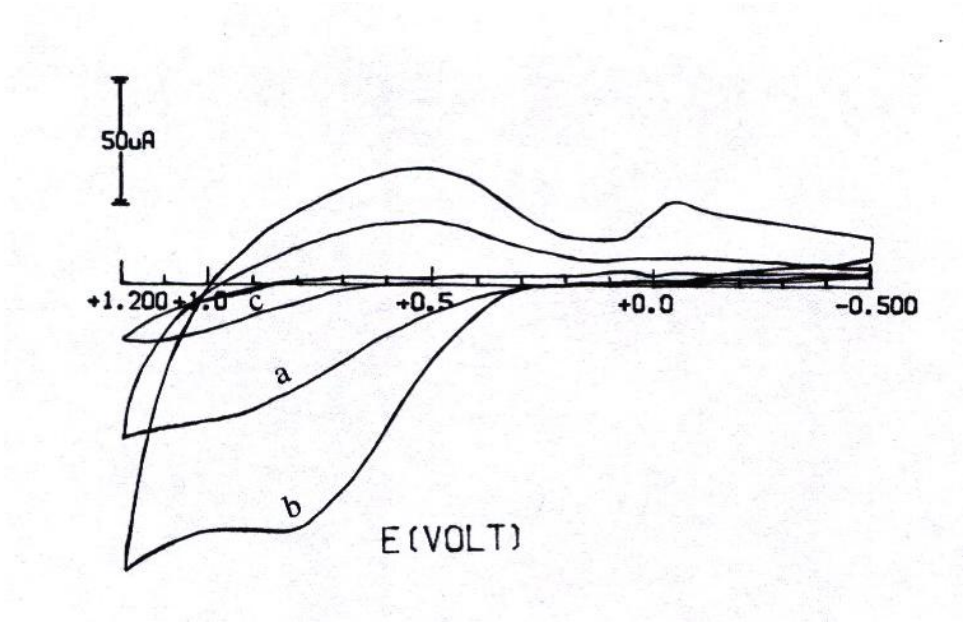

Figure 2b. Cyclic voltammogram of PMPy formed by 3 cycles in $TBAPF_6$/AcN and tested in $TBAPF_6$/AcN, $TBAPF_6$/AcN tested in $LiClO_4$/AcN, and $LiClO_4$/AcN tested in $TBAPF_6$/AcN, curves a, b, and c, respectively. Scan rate=50 $mV.s^{-1}$, E_i=-0.5 V, Ef=+1.2 V.

All three films were synthesized for 3 cycles in the monomer containing solution. The data of curves (a) and (c) show great similarities where an ill-defined oxidation peak is observed at around +0.8 V and a relatively broad one appear in the reverse reduction step.

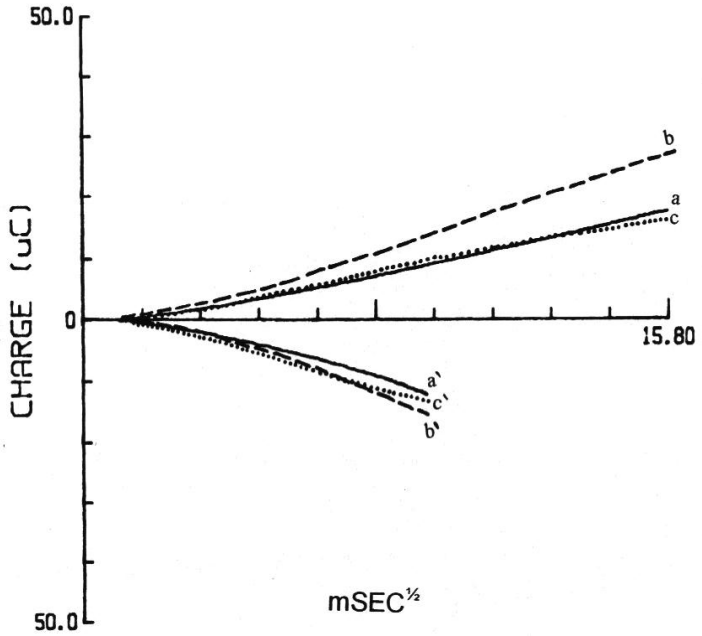

Figure 2c. Chronocoulometry experiment for PMPy films formed by repeated cycles (‴) 3 cycles, (---) 5 cycles, and (—) 10 cycles. a, b, c, and a`, b`, c` for the forward and reverse steps, respectively.

The current is noticeably higher in case of curve (a) compared to (c). The CV of curve (b) is distinctive in shape and currents passing in the oxidation and reduction cycles. One oxidation peak appears at +0.75 V and two relatively well-defined reduction peaks appear at +0.52 V and -0.05 V, respectively. Again, these data are explained in terms of the charge spacing created by the synthesis anion. Thus, "smaller" test anions should diffuse faster in films synthesized in rather "larger" anions. These data will be verified from the diffusion coefficient values estimated from the double-potential chronocoulometry experiments, Figure 2c.

The "charge spacing" effect caused by the type of electrolyte is more pronounced in the case of PMPy compared to PMT. This could be attributed to the differences in morphological structures, hydrophilic/hydrophobic characters, and difference towards oxygen sensitivity of the two films. The calculated *D* values for all PMPy films of different thicknesses synthesized and characterized in different electrolytes given in Table 2. The calculated values of diffusion coefficients, presented in Table 2, were close to those calculated by Grzeszczuk [18] for polypyrrole (10^{-7}-10^{-9} cm^2/s).

Table 2. Values of diffusion coefficients, *D* (cm^2/s), calculated from the double-potential experiments and using Cottrel equation (1). PMPy formed with different thickness (3, 5, 10 cycles) in AcN.

PMPy	3 Cycles	5 Cycles	10 Cycles
$TBAPF_6/TBAPF_6/AcN$*	$4.803x10^{-8}$	$4.677x10^{-8}$	$4.203x10^{-8}$
$TBAPF_6/LiClO_4/AcN$*	$6.091x10^{-8}$	$7.898x10^{-8}$	$9.822x10^{-8}$
$LiClO_4/LiClO_4/AcN$*	$1.353x10^{-8}$	$1.021x10^{-8}$	$1.343x10^{-8}$
$LiClO_4/TBAPF_6/AcN$*	$6.909x10^{-9}$	$3.556x10^{-9}$	$1.673x10^{-8}$
$LiClO_4/LiClO_4/H_2O$*	$8.915x10^{-9}$	$5.832x10^{-9}$	$4.443x10^{-9}$
$TBAPF_6/LiClO_4/H_2O$*	$9.466x10^{-9}$	$9.544x10^{-8}$	$6.587x10^{-8}$

* Synthesis electrolyte/test electrolyte/test solvent

The following observations could be noticed:

- The D values for PMPy are greatly smaller for thicker films when compared to those of PMT grown and tested in similar electrolytic conditions. In spite of the fact that PMPy is more hydrophilic in nature compared to PMT and its remarkable anion-exchange character, the charge exchange mechanism is not only governed by diffusion. Electronic charge transfer apparently contributes to the charge exchange and affects the calculated D values.
- The D values for PMPy are indepentent of the film thickness.
- The charge spacing effect is more manifested in the case of PMPy. This can be shown by comparing data of raw (1and 2) and (3 and 4).
- The effect of solvent used in the test solution is shown by comparing the data of raw (3 and 5). . For the same electrolyte used for both synthesis and testing steps, ClO_4^-, the D values are slightly larger when the test solvent is AcN than in case of it is H_2O. The possible explanation is the solvation of anion in aqueous medium that results in size increase.

3.5. Electrochemical polymerization and characterization of hetero-aromatics copolymers of MT and NMPy

The electropolymerization was conducted from solutions containing the following molar ratios of (MT:NMPy): (1:1), (1:2), (2:1), (1:9), and (9:1) and was achieved by repeated CV as described previously. Copolymers formed from these two monomers were not extensively mentioned in the literature [19].

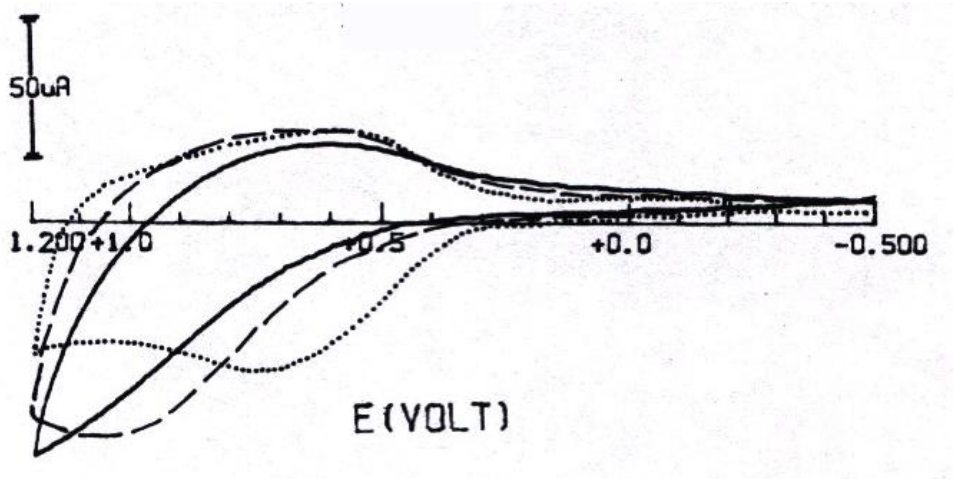

Figure 3a. Cyclic voltammogram of copolymer (formed by repeated cycles from feed solution (MT:NMPy, 1:2)/0.05 M $TBAPF_6$/AcN) in 0.05 M $TBAPF_6$/AcN. Films formed by 3 cycles (⁗), 5 cycles, (---), 10 cycles (—).

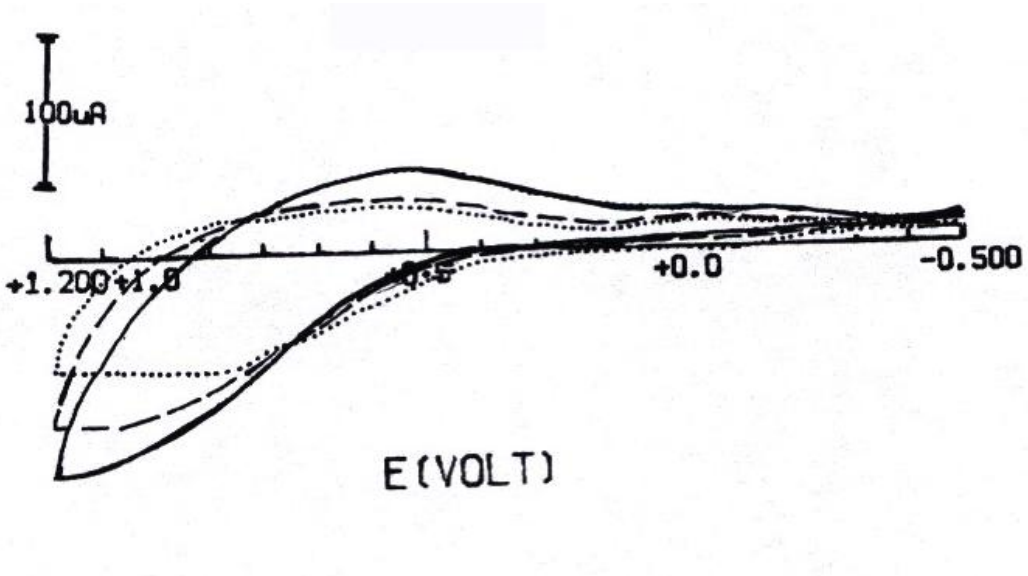

Figure 3b. Cyclic voltammogram of copolymer (formed by repeated cycles from feed solution (MT:NMPy, 1:9)/0.05 M $TBAPF_6$/AcN) in 0.05 M $TBAPF_6$/AcN. Films formed by 3 cycles (⁗), 5 cycles, (---), 10 cycles (—).

Moreover, the distinct behavior of each individual polymer suggests further investigation of copolymeric and bilayer structures as will be discussed later. The electrochemical features of the copolymerization of MT and NMPy are not similar to those of the individual monomers. Moreover, noticeable discrepancies are also noticed when changing the monomer ratios in solution. The incorporation of MT in the film catalyzes further film growth, copolymer (1:2), while the presence of NMPy in the film tends to hinder film growth, copolymer (1:1) and (2:1) (data are not shown). The electrochemical behavior of the formed copolymers was first examined by running the CV of the film in a monomer free solution. Thus Figures 3a, 3b and 3c show the electrochemical response of copolymer films prepared from comonomer solutions containing different feed ratios of the monomers.

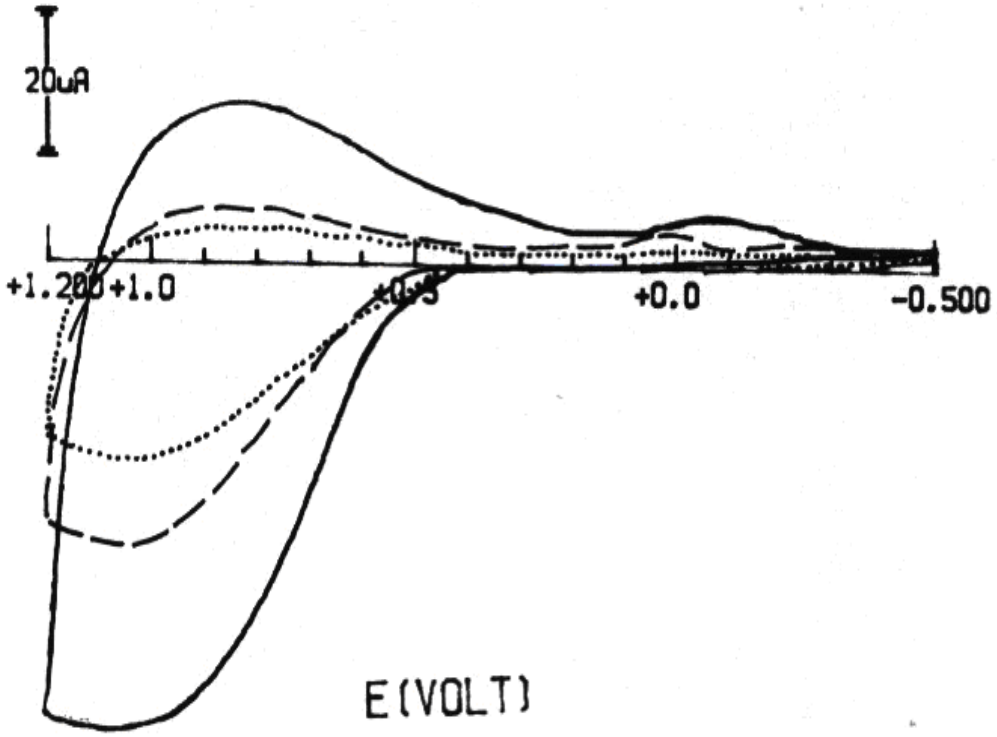

Figure 3c. Cyclic voltammogram of copolymer (formed by repeated cycles from feed solution (MT:NMPy, 1:9)/0.05 M $TBAPF_6$/AcN) in 0.05 M $TBAPF_6$/AcN. Films formed by 3 cycles (⋯), 5 cycles, (---), 10 cycles (—).

- For the CV of Figures 3a and 3c, the general shape of current-potential behavior shows predominance of MT moieties namely, the appearance of a well-defined anodic peak. As the film thickness increases, the anodic peak broadens and shifts to a more positive value.
- The predominance of NMPy moieties, on the other hand, is clear when impacting the CV of Figure 3b. The I-E response displays a rather "flat" CV with relatively lower currents passing during the forward and reverse scans.
- The diffusion coefficient values were calculated for films with different thickness prepared from different monomers feed ratios (Tables 3a, 3b, 4a and 4b).

Table 3a. Values of diffusion coefficients, D (cm^2/s), calculated from the double-potential experiments and using Cottrel equation (1). Copolymer (MT:NMPy) (1:2) formed with different thickness (3, 5, 10 cycles) in AcN.

Copolymer (1:2)	3 Cycles	5 Cycles	10 Cycles
$TBAPF_6/TBAPF_6/AcN$*	$1.061x10^{-7}$	$5.137x10^{-8}$	$4.595x10^{-8}$
$TBAPF_6/LiClO_4/H_2O$*	$9.858x10^{-9}$	$7.009x10^{-8}$	$1.293x10^{-8}$
$LiClO_4/LiClO_4/AcN$*	$2.641x10^{-9}$	$6.432x10^{-9}$	$1.190x10^{-8}$
$LiClO_4/LiClO_4/H_2O$*	$7.194x10^{-11}$	$3.142x10^{-9}$	$2.123x10^{-9}$

* Synthesis electrolyte/test electrolyte/test solvent.

Table 3b. Values of diffusion coefficients, D (cm^2/s), calculated from the double-potential experiments and using Cottrel equation (1). Copolymer (MT:NMPy) (2:1) formed with different thickness (3, 5, 10 cycles) in AcN.

Copolymer (2:1)	3 Cycles	5 Cycles	10 Cycles
$TBAPF_6/TBAPF_6/AcN$*	$1.919x10^{-8}$	$3.876x10^{-8}$	$2.435x10^{-8}$
$TBAPF_6/LiClO_4/H_2O$*	$5.141x10^{-9}$	$3.118x10^{-8}$	$4.146x10^{-8}$
$LiClO_4/LiClO_4/AcN$*	$7.611x10^{-10}$	$1.677x10^{-9}$	$1.659x10^{-9}$
$LiClO_4/LiClO_4/H_2O$*	$4.856x10^{-11}$	$8.573x10^{-11}$	$1.152x10^{-11}$

* Synthesis electrolyte/test electrolyte/test solvent.

Table 4a. Values of diffusion coefficients, D (cm^2/s), calculated from the double-potential experiments and using Cottrel equation (1). Copolymer (MT:NMPy) (1:9) formed with different thickness (3, 5, 10 cycles) in AcN.

Copolymer (9:1)	3 Cycles	5 Cycles	10 Cycles
$TBAPF_6/TBAPF_6/AcN$*	$7.601x10^{-8}$	$4.853x10^{-8}$	$8.405x10^{-8}$
$TBAPF_6/LiClO_4/H_2O$*	$5.429x10^{-8}$	$1.431x10^{-8}$	$3.226x10^{-8}$

* Synthesis electrolyte/test electrolyte/test solvent.

Table 4b. Values of diffusion coefficients, D (cm^2/s), calculated from the double-potential experiments and using Cottrel equation (1). Copolymer (MT:NMPy) (9:1) formed with different thickness (3, 5, 10 cycles) in AcN.

Copolymer (9:1)	3 Cycles	5 Cycles	10 Cycles
$TBAPF_6/TBAPF_6/AcN$*	$1.026x10^{-8}$	$1.638x10^{-8}$	$8.993x10^{-8}$
$TBAPF_6/LiClO_4/H_2O$*	$6.744x10^{-11}$	$3.432x10^{-9}$	$1.297x10^{-8}$

* Synthesis electrolyte/test electrolyte/test solvent.

The following observations could be made:

- For all films studied (except for that prepared from a monomer feed (MT:NMPy) (9:1)/TBAPF6/AcN and tested in LiClO4/H2O), there is no distinct trend in the D values with film thickness (the same trend observed for homo-PMPy films). On the other hand, for the "(9:1) copolymer" synthesized in TBAPF6/AcN and tested in LiClO4/H2O, the D values increases with thickness with a noticeable two orders of magnitude. Similar trend was observed in case of homo-PMT films.
- The presence of NMPy in the polymer chain results in relative lowering of the D values compared to those of homo-PMT films, namely, for thicker films. On the other hand, the presence of MT in the polymer chains results in relative lowering of the D values for films tested in aqueous solution compared to those of homo-PMPy.

3.6. Electrochemical polymerization and characterization of PMT-PMPy bilayer films

Bilayered structures of conducting polymers where two homopolymeric layers deposit successively onto a solid substrate were studied. A layer of PMT (or PMPy) was electrochemically deposited on Pt disc by cycling the potential with scan rate=50mV.s^{-1} in 0.05 M monomer (MT or NMPy) / 0.05 $TBAPF_6$ / AcN for three cycles. This was followed by similarly depositing a layer of PMPy (or PMT). Figures 4a and 5a show repeated CV (3 cycles) for the deposition of PMPy over PMT and PMT over PMPy, respectively.

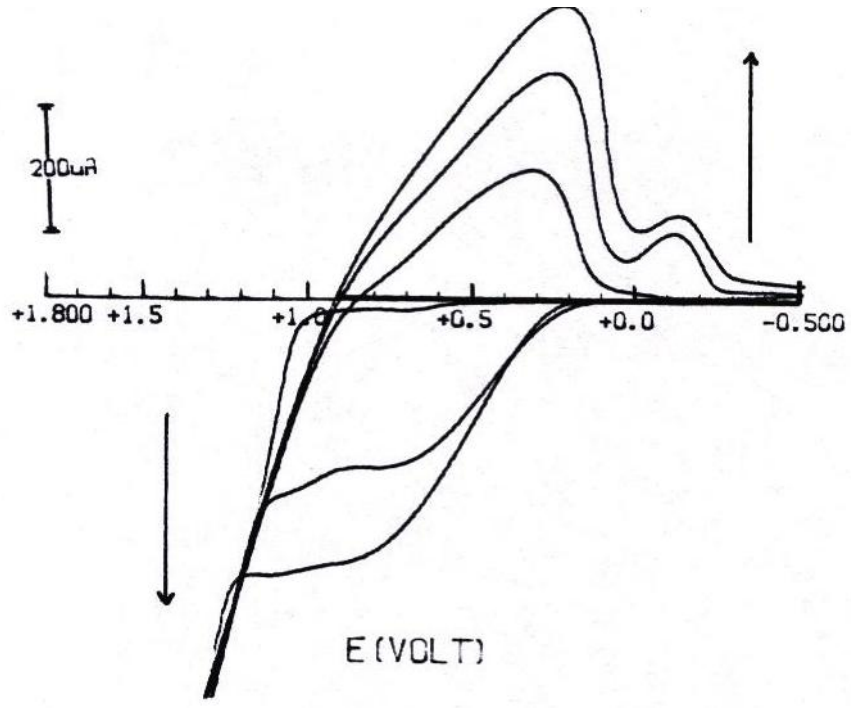

Figure 4a. Repeated cyclic voltammogrames for the formation of PMPy over PMT (formed by 3 cycles in 0.05 M MT, 0.05 M $TBAPF_6$ in AcN), Electrolyte: 0.05 M NMPy, 0.05 M $TBAPF_6$ in AcN, scan rate=100 mV.s^{-1}, E_i=-0.5 V, E_f=+1.8 V for 3 cycles.

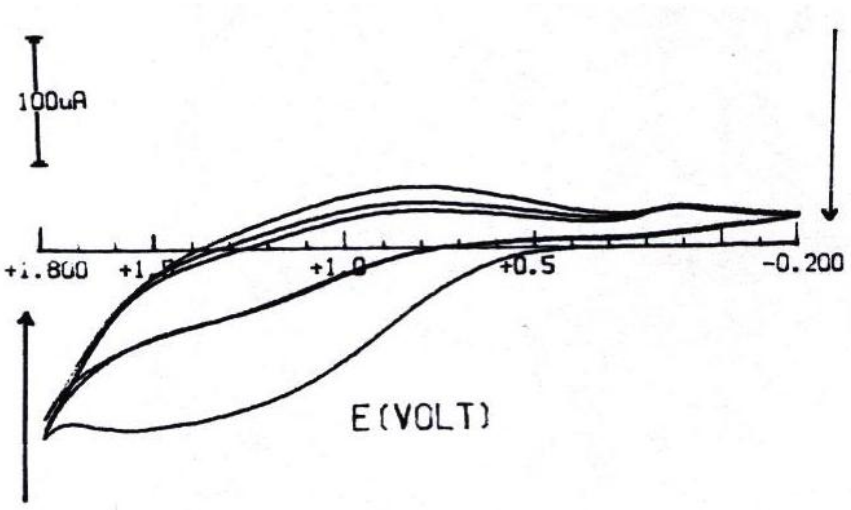

Figure 5a. Repeated cyclic voltammogrames for the formation of PMT over PMPy (formed by 3 cycles in 0.05 M NMPy, 0.05 M $TBAPF_6$ in AcN), Electrolyte: 0.05 M MT, 0.05 M $TBAPF_6$ in AcN, scan rate=100 $mV.s^{-1}$, E_i=-0.2 V, E_f=+1.8 V for 3 cycles.

The current passing is relatively higher when PMT is the underlying layer. Moreover, the current increases for successive cycles (Figure 4a) indicating film thickness with appreciable conductivities. While the current decreases for successive cycles in Figure 5a. These results indicate that the inner layer of bilayer polymer either catalyzes further growth of successive polymer layers or prevents further film deposition. The polymer bilayers, PMT/PMPy and PMPy/PMT (inner layer/outer layer) deposited on Pt, were then characterized in monomer free solutions by CV and the corresponding diffusion coefficients were also be determined. Figure 4b and 5b show the CV of PMT/PMPy and PMPy/PMT, respectively.

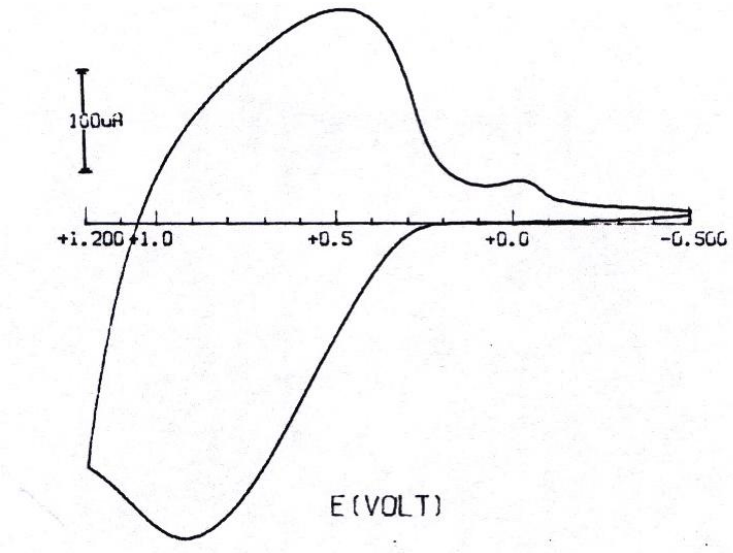

Figure 4b. Cyclic voltammogram of PMPy over PMT (each formed by 3 cycles in 0.05 M monomer, 0.05 M $TBAPF_6$ in AcN), in 0.05 M $TBAPF_6$/AcN, scan rate=50$mV.s^{-1}$, E_i=-0.5 V, E_f=+1.2 V.

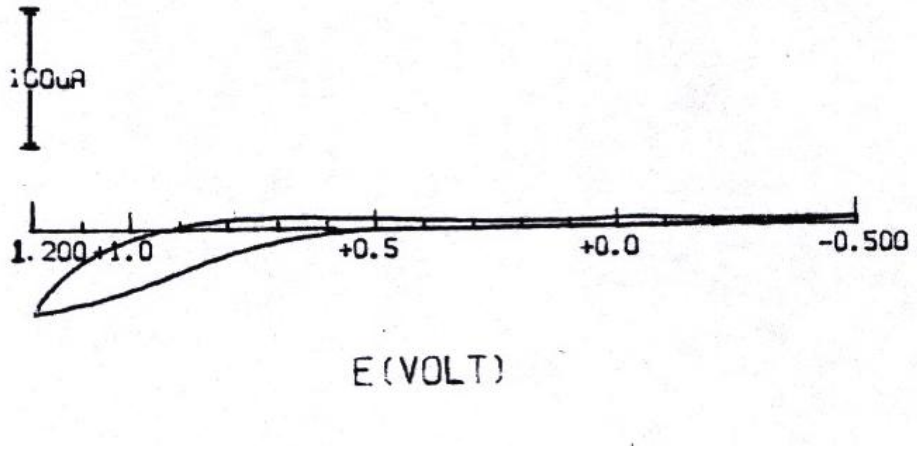

Figure 5b. Cyclic voltammogram of PMT over PMPy (each formed by 3 cycles in 0.05 M monomer, 0.05 M $TBAPF_6$ in AcN), in 0.05 M $TBAPF_6$/AcN, scan rate=50mV.s^{-1}, E_i=-0.5 V, E_f=+1.2 V.

In the case of PMT/PMPy bilayer, PMPy outer layer influence on the redox process of the inner PMT layer indicates that the charge compensating counter ions needed for the inner layer were provided through the outer PMPy layer. This is in good agreement with the ionic exchange ability of PMPy [20]. On the other hand, the CV of Figure 5b shows that the outer layer of PMT does not affect the redox behavior of PMPy but rather reduces the current passing. This is explained by the less ability of PMT to deliver ionic species to the inner layer. These results indicate that the oxidation of the inner layer is limited by charge diffusion in case of PMPy (outer layer) and by charge hopping in case of PMT (outer layer). Moreover, electrochemical response is predominantly revealing the inner layer behavior. The above results are in agreement with the estimated *D* values from the double-potential step experiments as indicated in Table 5 which showed that the diffusion coefficient in case of Pt/PMT/PMPy is larger than in case of Pt/PMPy/PMT in all electrolytes.

Table 5. Values of diffusion coefficients, *D* (cm^2/s), calculated from the double-potential experiments and using Cottrel equation (1). Conducting bilayers, each layer is formed by 3 cycles.

Bilayer	$TBAPF_6$/$TBAPF_6$/AcN*	$LiClO_4$/$LiClO_4$/AcN*	$LiClO_4$/$LiClO_4$/H_2O*
Pt/PMT//PMPy	5.007×10^{-8}	4.114×10^{-8}	5.265×10^{-9}
Pt/PMPy//PMT	1.970×10^{-10}	2.406×10^{-8}	4.777×10^{-11}

3.7. FTIR of homopolymer and copolymer films

The current infrared investigations were aimed to ascertain the formation of the copolymers and to identify the presence of each repeat unit in the chain, namely MT and NMPy. Figures 6a, 6b show the FTIR spectra, in the range of (4000-400 cm^{-1}), of KBr pressed pellets of PMT and PMPy, respectively.

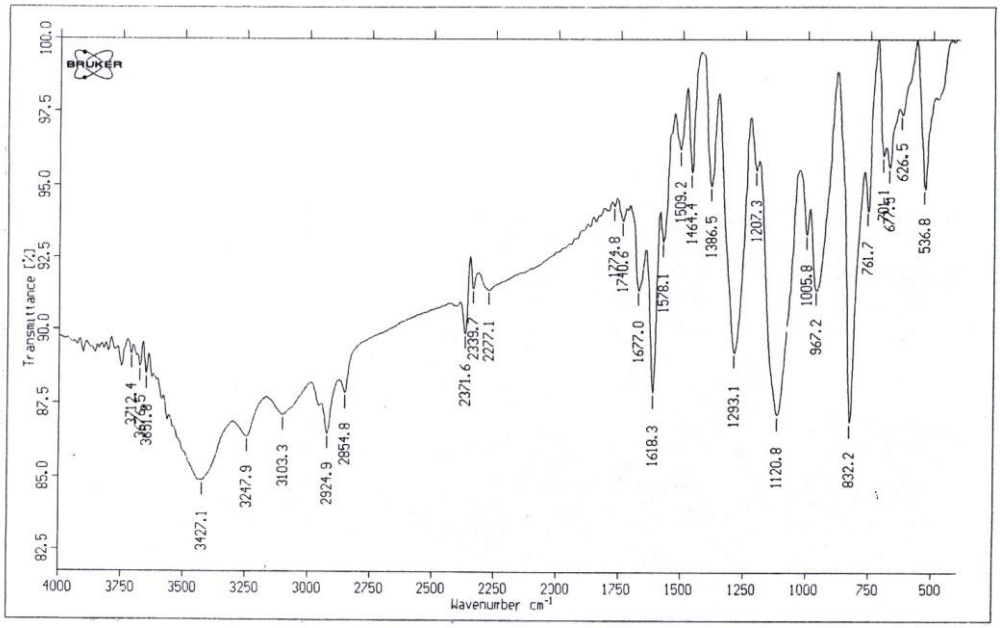

Figure 6a. FTIR spectrum for PMT prepared from 0.05 M MT/0.05 M $TBAPF_6$/AcN by applying +1.8 V

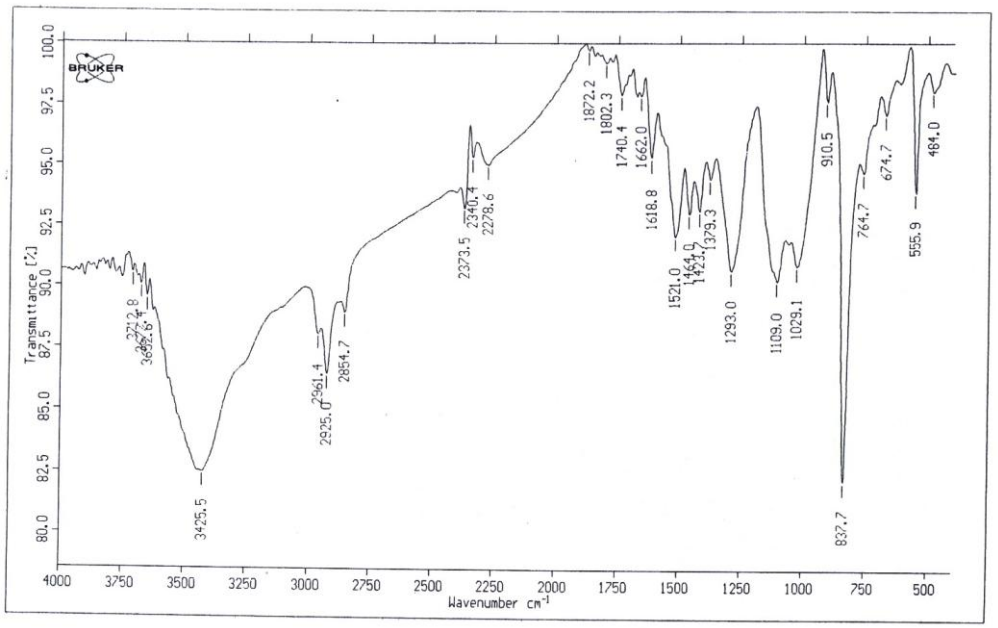

Figure 6b. FTIR spectrum for PMPy prepared from 0.05 M NMPy/0.05 M $TBAPF_6$/AcN by applying +1.8 V

For PMT, vibration peak due to ring stretching was observed at 1464.4 cm^{-1}. The methyl deformation vibration peak was observed at 1386.5 cm^{-1}. Strong doping induced vibration peak was observed at 1293.1 cm^{-1}. For PMPy, weak bands attributable to aromatic and aliphatic CH stretching are observed around 3000 cm^{-1} such as bands at 2961.4 cm^{-1} (ring CH stretching), 2925 cm^{-1} (methyl CH stretching). Bands due to PMPy backbone vibrations appear below 1600 cm^{-1} for example: 1521

and 1293 cm^{-1} are assigned to C=C and C–N vibrations, respectively. These results are in a good agreement with those published earlier [21, 22]. FTIR spectrum for a copolymer of MT and NMPy (1:1) was also measured as shown in Figure 6c.

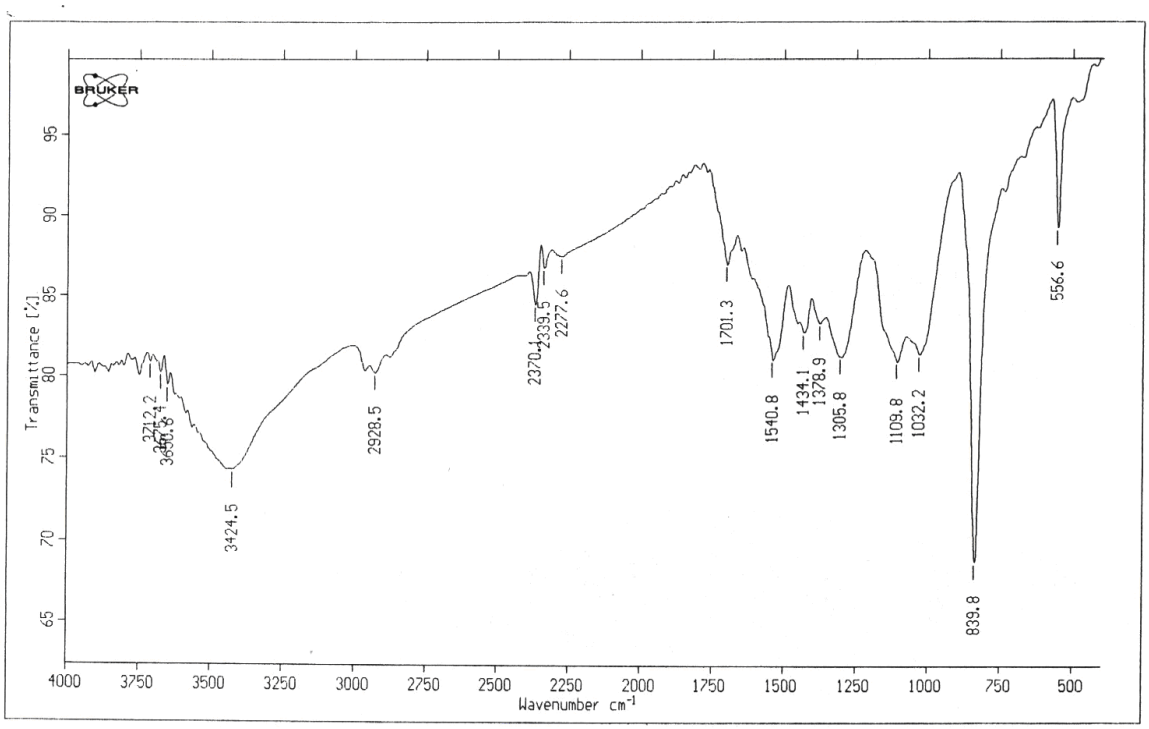

Figure 6c. FTIR spectrum for copolymer prepared from a feed solution containing (MT:NMPy, 1:1)/0.05 M $TBAPF_6$/AcN by applying +1.8 V

The spectrum shows that MT and NMPy are both incorporated into the copolymer. FTIR spectrum of the copolymer was compared to those of PMT and PMPy. Peaks at 1434.1, 1305.8 cm^{-1} which are assigned to ring stretching and C–N stretch of PMT and PMPy, respectively indicate that the two monomers are incorporated into the copolymer. One of the features of the FTIR spectrum of PMPy is a splitted peak at 1109.8, 1032 cm^{-1} Figure 6b. The same peak was clearly identified in the case of the copolymer, Figure 6c.

3.8. Thermogravimetric analysis

Thermal behavior was necessary to investigate the thermal stability of the polymer films and how it can be affected by copolymerization. Figure 7 shows TGA (a) and DTG (b) data for PMT, PMPy,and copolymer (1:1). TGA curves were plotted as weight losses as a function of temperature, while DTG curves were plotted to express the rate of weight change as a function of temperature. Comparing the data of Figure 7

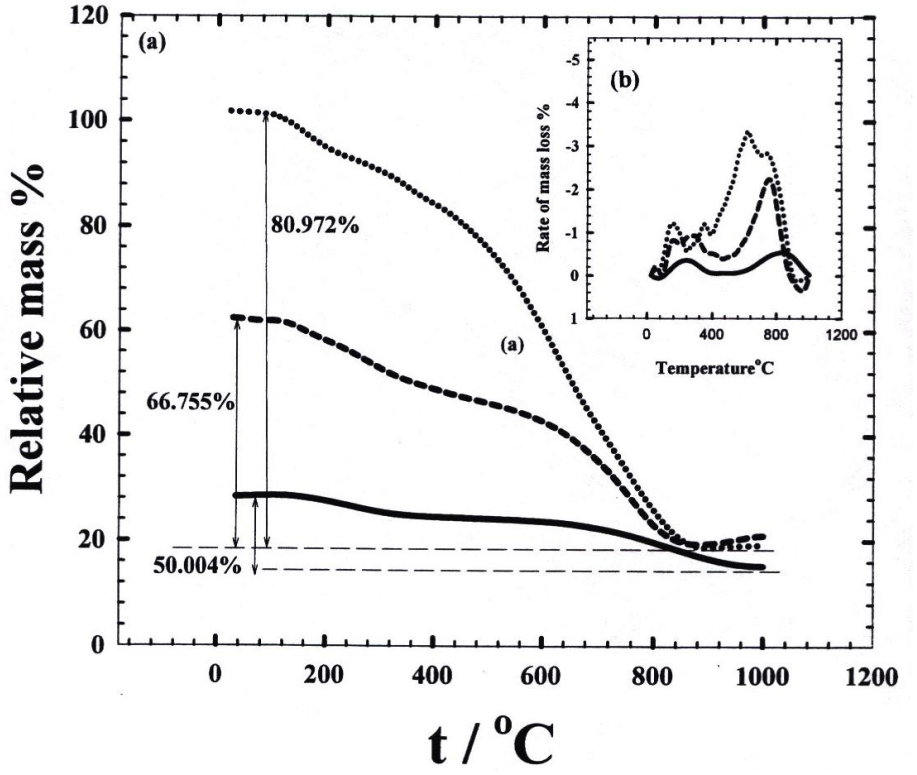

Figure 7. TGA (a) and DTG (b) data for PMPy (—), copolymer (1:1) (----) and PMT (**....**).

The following observations could be withdrawn:

- The thermal behavior of PMT shows a sharp and large inflection at 150°C. At this stage, about 8.390% of weight loss of PMT is noticed. This could be justified by the considerable solvent uptake of the polymer film during the synthesis step. A series of successive peaks appears at 320°C, 580°C. The weight loss for these temperatures transitions are 8.691%, 39.047% respectively. This weight loss could be attributed to the reorganization of the polymer chains.
- For PMPy, a distinct thermal behavior could be noticed. The weight loss due to the solvent loss is relatively smaller compared to that for PMT and can not be noticed. This is because of the more hydrophobic nature of PMT which allows the incorporation of much more of the organic solvent during synthesis.
- For the copolymer (1:1), the total weight loss (66.755%) is smaller than that for PMT (80.972%) and larger than that for PMPy (50.004%). We can conclude that the incorporation of NMPy will increase the thermal stability of the copolymer compared to PMT.

3.9. Scanning electron microscope

Scanning electron micrographs of PMT thin films showed that the surface is regular and homogeneous and does not show the spheroid-like defects of other conducting polymers [23]. A porous structure was also expected for relatively thick films as was found earlier with similar

polymeric classes [24]. Scanning electron micrographs of PMPy showed that the surface consists of fine microspheroidal grains and the surface of PMPy is relatively smooth [25].

MT and NMPy have been copolymerized electrochemically to form thin electronically conducting copolymer films. The morphology of the films was investigated by SEM. Two samples were prepared, the first is a copolymer film that was deposited at a platinum substrate from feed solution containing (MT:NMPy) (1:2) / $TBAPF_6$ / AcN, Figure 8a. The second is a copolymer film that was deposited from feed solution containing (MT:NMPy) (9:1) / $TBAPF_6$ / AcN, Figure 8b. Both samples were prepared by applying + 1.8 V to the platinum substrate for 1 min.

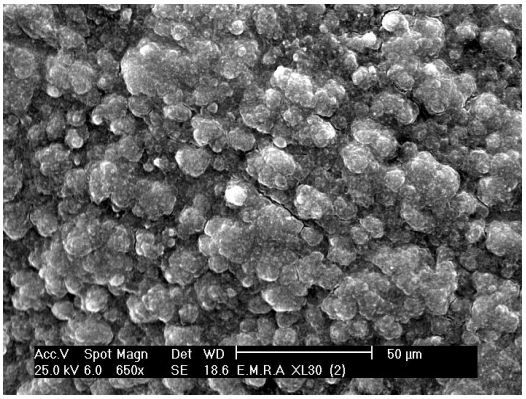

Figure 8a. SEM for copolymer prepared from a feed solution containing (MT:NMPy, 1:2)/ 0.05 M $TBAPF_6$/AcN, by applying + 1.8 V for 1 min with magnification 650 times.

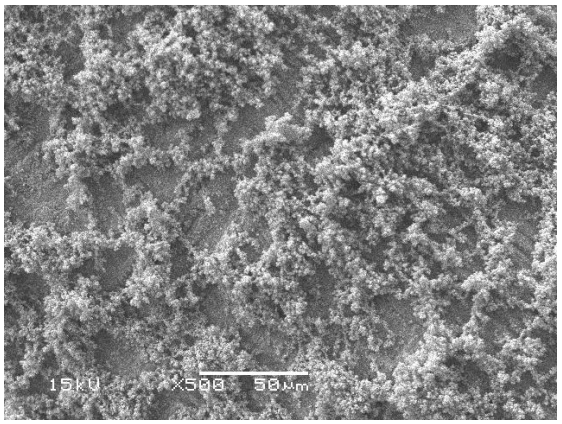

Figure 8b. SEM for copolymer prepared from a feed solution containing (MT:NMPy, 9:1)/ 0.05 M $TBAPF_6$/AcN, by applying + 1.8 V for 1 min with magnification 650 times.

As could be noticed for the copolymer (1:2), Figure 8a, most of the surface consists of one phase which is smooth and pocesses microspheroidal grains. We can conclude that the surface morphology of the copolymer thus formed is predominantly showing PMPy characteristics. On the other hand, for the copolymer (9:1), Figure 8b, more porous features of the surface can be identified.

This is in agreement with the previously mentioned literature showed that the porosity of the copolymer surface is increased with increasing MT content in the feed solution [26].

Bilayered polymer films were also investigated by SEM. Figure 8c shows the scanning electron micrograph for PMPy formed over PMT.

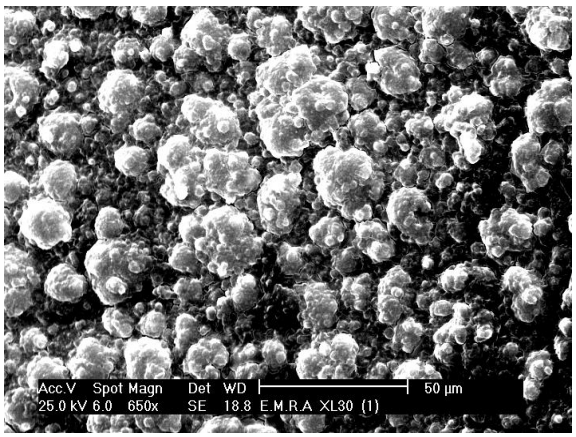

Figure 8c. SEM for PMPy over PMT, each prepared from 0.05 M monomer/ 0.05 M $TBAPF_6$/AcN, by applying + 1.8 V for 1 min with magnification 650 times.

Two phases can be observed, the inner phase which is more porous, corresponding to PMT, and the outer phase which is denser, corresponding to PMPy. From the surface study, it can be concluded that the predominant behavior is for the inner layer.

4. CONCLUSION

It is possible to prepare conducting homo-, bi-, and co-polymers from MT and NMPy monomers over solid substrates. The electrochemical characterizations were carried out by CV, CC. The *D* values were estimated. It was found that for PMT, film thickening results in an increase in doping level that reflects the observed slight increase in *D* values. The hydrophobic nature of the surface of the polymer hinders the diffusion of the solvated anions when using water as a characterization solvent. Increase in charge to size ratio of test anion compared to that of synthesis anion shows slight increase in *D* values. For PMPy, the *D* values are smaller when compared to those of PMT grown and tested in similar electrolytic conditions and it is independent of the film thickness. The charge spacing effect is more manifested in the case of PMPy. For all copolymers studied, except for that prepared from a monomer feed (9:1)/$TBAPF_6$//$LiClO_4$/H_2O, there is no distinct trend in the *D* values with film thickness. On the other hand, for the "copolymer (9:1)" in $LiClO_4$/H_2O, the *D* values increases with thickness with a noticeable two orders of magnitude. Nearly similar trend was observed in case of homo-PMT films. For conducting bilayers, the inner layer influences the redox process of the bilayer. This can be shown from the CV of formation, CV of characterization and the calculated *D* values.

References

1. P.G Pickup, W. Kutner,C.R Leidner, R.W Murray, *J Am Chem Soc*, 106(7) (1984) 1991-1998.
2. C.R Leidner, P. Denisevich, K.W Willman, R.W Murray, *J Electroanal Chem*, 164(1) (1984) 63-78.
3. W Torres, M.A Fox, *Chem. Mate*, 2(3) (1990) 306-311.
4. A.R Hillman, E.F Mallen, *J Electroanal Chem*, 309(1-2) (1991) 159-171.
5. A.R Hillman, E.F Mallen, *Electrochim Acta*, 37(10) (1992) 1887-1896.
6. D.N Upadhyay, S. Bharathi, V.Yegnaraman, G.P Rao, *Sol. Energy Mater. Sol. Cells*, 37(3-4) (1995) 307-314.
7. N.O Pekmez, E. Abacı, K.Cınkıllı, A.Yağan, *Prog Org Coat*, 65(4) (2009) 462-468.
8. Q. Pei , O.I Österholm, J. Laakso, *Polymer*, 34(2) (1993) 247-252.
9. M.Lu, X. Li, H.Li, *Mater Sci Eng A*, 334(1-2) (2002) 291-297.
10. M. Ak, L. Toppare, *Mater Chem Phys*,114(2-3) (2009)789-794.
11. H.S.O Chan, E.T Kang, K.G Neoh, K.L Tan, B.T.G Tan, Y.K Lim. *Synth Met*, 30(2) (1989) 189-197.
12. P.Novák , W. Vielstich, *J Electroanal Chem*, 300(1-2) (1991) 99-110.
13. N.F Atta, A. Galal, M.F El-Kady, *Anal. Biochem*, 400 (2010) 78-88.
14. N.F Atta, A. Galal , R.A Ahmed, *Bioelectrochem*, 80 (2011) 132-141.
15. A.J Bard, L.R Faulkner, *Electrochemical methods, Fundamental applications*, (2001).
16. K Jüttner, R.H.J Schmitz, A Hudson, *Electrochim Acta*, 44 (24) (1999) 4177-4187.
17. Y Tezuka, K Aoki, T Ishii, *Electrochim Acta*, 44 (1999) 1871-1877.
18. M. Grzeszczuk, *Polish J. Chem*., 78 (2004) 1423–1429.
19. J.P Ferraris, D.J Guerrero, *Recent advances of heteroaromatic copolymers*, (1998) 259-276.
20. P. Burgmayer, R.W Murray,*J Electroanal Chem*,147(1-2) (1991) 339-344.
21. D.H Park, B.H Kim, M.K Jang, K.Y Bae, S.J Lee, J. Joo, *Synth Met*, 153(1-3) (2005) 341-344.
22. G.Erdogdu, A.E Karagözler, *Talanta*, 44(11) (1998) 2011-2018.
23. G.Tourillon, F. Garnier, *J Electroanal Chem*,135(1) (1982) 173-178.
24. R.H.M Van de leur, *Synth Me*, 51(1-3) (1992) 69-74.
25. W. Su, J.O Iroh, *Electrochim Acta*, 44(19) (1999) 3321-3332.
26. B.Fabre, F. Kanoufi, J. Simonet, *J Electroanal Chem*, 434(1-2) (1997) 225-234.